Synthesis and Electrochemical Study of $CoNi_2S_4$ as a Novel Cathode Material in a Primary Li Thermal Battery

Kyriakos Giagloglou,[a] Julia L. Payne,[a] Christina Crouch,[b] Richard K. B. Gover,[b] Paul A. Connor,[a] and John T. S. Irvine[a,*,z]

[a]*School of Chemistry, University of St. Andrews, North Haugh, St. Andrews, Fife KY16 9ST, United Kingdom*
[b]*AWE Plc, Aldermaston, Reading RG7 4PR, United Kingdom*

In this work $CoNi_2S_4$ was investigated as a candidate cathode material for Li thermal batteries. The $CoNi_2S_4$ was synthesized by a solid state reaction at 550°C in a sealed quartz tube. Neutron powder diffraction was utilized to confirm normal spinel structure up to 200°C, however, there was cation disorder above this temperature. The electrochemical properties of the batteries were investigated at 500°C by galvanostatic discharge to elucidate the mechanism and the products NiS, Co_3S_4 and Co_9S_8 of the discharge mechanism were confirmed using powder X-ray diffraction. $CoNi_2S_4$ exhibits two voltage plateaus vs $Li_{13}Si_4$ at 500°C, one at 1.75 V and the second at 1.50 V. $CoNi_2S_4$ has an overall capacity of 318 mA h g^{-1} from OCV 2.58 V to 1.25 V vs $Li_{13}Si_4$ which is comparable to that of the well-known metal disulfides.
 [DOI: 10.1149/2.1171709jes]

Manuscript submitted March 9, 2017; revised manuscript received May 5, 2017. Published July 25, 2017.

Today the human society and technology progress in electric vehicles, medical equipments, military applications and space technology require power systems with high energy, safety and long shelf – life characteristics. There are different kind of power systems such as supercapacitors, fuel cells and thermal batteries for this goal. Thermal batteries are electrochemical devices that offer a direct conversion of chemical energy to electrical energy by an electrochemical oxidation-reduction reaction at high temperature (>300°C) utilizing a molten salt electrolyte. Thermal batteries are primary batteries which find use in a number of applications as they are known for their long shelf life and ability to be discharged at particularly high rates when compared to other types of batteries.[1] A key component of thermal batteries is the halide salt electrolyte that is a solid at ambient temperatures which gives the cells their long life but melts in the 300–500°C region.[2] This solid – liquid phase transition leads to the electrolyte becoming ionically conductive and allowing the ions to transfer between the anode and the cathode. Thermal batteries typically use a lithium alloy as the anode, a halide salt eutectic as the electrolyte, an insulating porous material as the separator and a transition metal sulfide as the cathode. The $Li_{13}Si_4$ alloy is often used as the anode as the lithium diffusion in silicon (10^{-8} cm^{-2} s^{-1}) is greater than in other alloys[3] and has moisture stability as well as it staying solid at the operating temperature. The discharge reaction of $Li_{13}Si_4$ to Li_7Si_3 at a potential of 0.157 V against Li metal at 415°C corresponds to a capacity of 485 mA h g^{-1}.[4] The electrolyte that has been used in this work is the lithium chloride – potassium chloride eutectic which has a melting point of around 354°C and requires a minimum of 35 wt% MgO as a separator.[5] The most common transition metal disulfides to be used as cathodes are FeS_2, NiS_2 or CoS_2 and all of these materials exhibit a potential of ~ 1.70 V vs $Li_{13}Si_4$ at the beginning of their discharge but also have further electrochemical transitions to complete the reduction to the transition metal.[6]

The improvement in Li thermal batteries will come through the investigation of novel and better cathodes. The best cathode for use in thermal batteries should have a high voltage (>3 V) and a high capacity. It should also be a good electronic conductor and have a low solubility in the chosen molten salt electrolytes. It is ideal if the cathode exhibits multiphase discharge (and not intercalation) as this enables better voltage control, providing a constant power for longer than if an intercalation compound was used.[7,8]

Recently, $CoNi_2S_4$ has been used as an electrode material for supercapacitors and exhibits promising electrochemical performance, such as a high specific capacitance, an excellent rate capability, a long cycling life and a high energy density.[9–11]

*Electrochemical Society Member.
[z]E-mail: jtsi@st-andrews.ac.uk

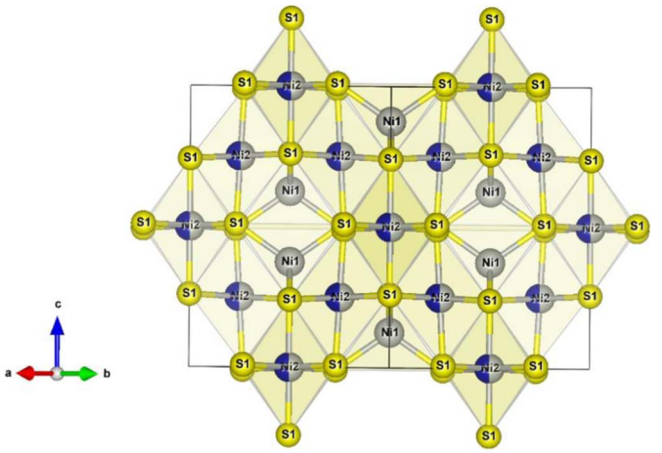

Figure 1. Crystal structure of an inverse spinel $CoNi_2S_4$. Yellow atoms are sulfur, gray atoms are nickel and blue atoms are cobalt.

Thio-spinels with the general formula $A^{2+}B^{3+}{}_2S^{2-}{}_4$ have the sulfur anions arranged in a cubic close-packed lattice and the cations A^{2+} and B^{3+} occupy the octahedral and tetrahedral sites in the lattice. The B^{3+} cations occupy half of the octahedral holes, while the A^{2+} ions occupy one-eighth of the tetrahedral holes. $CoNi_2S_4$ adopts an inverse spinel structure as shown in Figure 1. Here the Co cations and half of the Ni cations occupy octahedral sites, while the remaining Ni cations occupy tetrahedral sites.[12]

Although the synthesis of $CoNi_2S_4$ has previously been reported by Knop and Huang, their solid state synthesis of $CoNi_2S_4$ involved multiple firings at temperatures from 500°C to 600°C for 3 days, 2 days, 5 days, 6 days, 1 month and 20 days, i.e. a total of 63 days. The long duration of this reaction is not practical, so we decided to explore a variety of synthetic conditions with the aim to synthesize the material in a shorter time frame. This would enable us to carry out our synthesis and electrochemical testing more efficiently.

The aim of this work is to synthesize and characterize $CoNi_2S_4$ and test it as a cathode in a Li thermal battery.

Experimental

$CoNi_2S_4$ was synthesized by a solid state reaction in a sealed quartz tube to prevent oxidation of the sample during synthesis. 0.77 g of nickel (Aldrich,-100mesh, 99%), 0.38 g of cobalt (Alfa Aesar, -325mesh, 99.5%) and 0.83 g of sulfur (Alfa Aesar,-100mesh, 99.5%)

Table I. Experimental conditions for the synthesis of $CoNi_2S_4$.

1st Firing	Ball milling	2nd Firing	Ball milling	3rd Firing	Single phase
400°C for 24 hours	1 hour in air with acetone	400°C for 168 hours	1 hour in air with acetone	400°C for 24 hours	No
480°C for 24 hours	1 hour in argon	480°C for 168 hours	1 hour in argon	480°C for 24 hours	No
480°C for 24 hours	grinding in mortar and pestle in glove box	480°C for 168 hours	grinding in mortar and pestle in glove box	480°C for 24 hours	No
500°C for 24 hours	1 hour in air with acetone	500°C for 168 hours	1 hour in air with acetone	500°C for 24 hours	No
550°C for 34 hours	4 hours in argon	550°C for 156 hours	No	No	Yes

powders were weighed out and mixed in a mortar and pestle in air and then sealed into an evacuated (10^{-3} mbar) quartz tube. The tube was heated in a tube furnace with a heating and cooling rate of 1°C min^{-1} with the duration, temperature and number of firings used in the synthesis presented in Table I. Between each firing the sample was ball milled under argon for 4 hours to achieve homogeneity. Powder X-ray diffraction analysis was conducted in order to identify the crystalline phases present using a Panalytical Empyrean diffractometer in Bragg-Brentano geometry with a Ge(220) monochromator and Cu $K\alpha_1$ radiation ($\lambda = 1.5405$ Å). Data were collected in the 10° to 100° 2θ range for 1 hour, with a step size of 0.017° and a time per step of 0.68 seconds. Powder neutron diffraction data were collected on the High Resolution Powder Diffractometer (HRPD) at the ISIS neutron source, Rutherford Appleton Laboratory, UK. Rietveld refinement was carried out using General Structure Analysis System (GSAS).[13,14] Scanning electron microscopy was carried out using a Jeol JSM-5600 to study the morphology and composition of the cathode powder.

The composite cathode pellet (diameter 13 mm) for high temperature electrochemical investigation was made by mixing 75 wt% $CoNi_2S_4$ (0.15 g) with 25 wt% Super P Carbon (0.05 g). The anode pellet was made by mixing 75 wt% $Li_{13}Si_4$ (Lithium Rockwood) (0.15 g) and 25 wt% LiCl-KCl electrolyte (0.05 g). Thermal cells were assembled in an argon-filled glove box by stacking a microporous separator pellet containing 45 wt% MgO and 55 wt% LiCl-KCl eutectic electrolyte (0.2 g) (Sigma Aldrich 99.99%) onto an anode pellet and then the cathode pellet on the top. The amount of anode (0.15 g) is in excess to keep the discharge on the first anode plateau for the amount of cathode used. To prevent movement all three pellets were contained in a ceramic cup with graphite foil as the current collectors top and bottom. The resulting cell was placed into a Swagelok sample holder, allowing the measurements to be carried out sealed and heated in an electric furnace. The cells were tested at 500°C and were investigated electrochemically by a Maccor battery tester model 5300 by galvanostatic discharge. The experimental capacity was calculated using the Maccor software and then this was converted to *x*, the moles of lithium ions per moles of formula unit. All voltages are reported compared to the anode as a voltage reference i.e. all voltages are vs $Li_{13}Si_4$.

Results and Discussion

Cathode material characterization.—The crystalline products obtained from the reactions between cobalt, nickel and sulfur powders were studied by powder X-ray diffraction (PXRD) as presented in Figure 2. At 400°C the sample was fired 3 times and ball milled twice and was not single phase. At 480°C the sample was fired 3 times and ball milled twice in argon and was not single phase. Then at 480°C the sample was fired 3 times and ground in a mortar and pestle in glove box but was not single phase. The reactions at carried out at 480°C show an improved phase purity with respect to the reactions carried out at 400°C. At 500°C the sample was fired 3 times and ball milled twice and was not single phase. From our experiments, the best synthetic conditions for the synthesis of $CoNi_2S_4$ were found to be synthesizing the sample in 8 days with 2 firing steps (at temperature of 550°C) by using ball milling in argon as an intermediate step, as outlined in Table I. The red line in Figure 2 shows that $CoNi_2S_4$ was identified as a single phase and the cell parameters ($\alpha = 9.4239(8)$ Å) and space group $Fd\bar{3}m$ were determined using the WinXPOW software. The morphology and the shape of the crystallites of $CoNi_2S_4$ was investigated by SEM and are presented in Figure 3. The size of the crystallites ranges from 1 to 5 μm and the shape of crystallites corresponds to the shape of the spinel structure.[15,16] EDX analysis confirms the elemental analysis of $CoNi_2S_4$ as the expected cobalt 15 at%, nickel 29 at% and sulfur 56 at%.

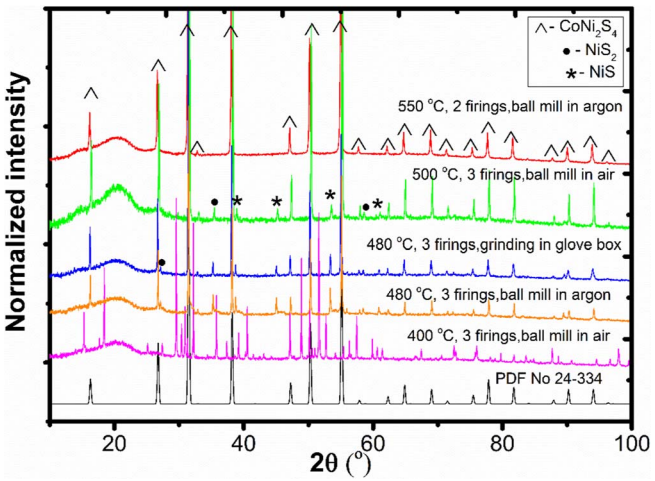

Figure 2. PXRD data of $CoNi_2S_4$ (using different synthetic conditions) compared to the simulated diffraction pattern of $CoNi_2S_4$ using the published crystallographic model[12] (black line). The broad peak at around 20° is from the protective air sensitive film which is used during data collection.

As Co^{2+} and Ni^{3+} are isoelectronic, it is impossible to distinguish between the possible Co and Ni ordering using X-ray diffraction. The

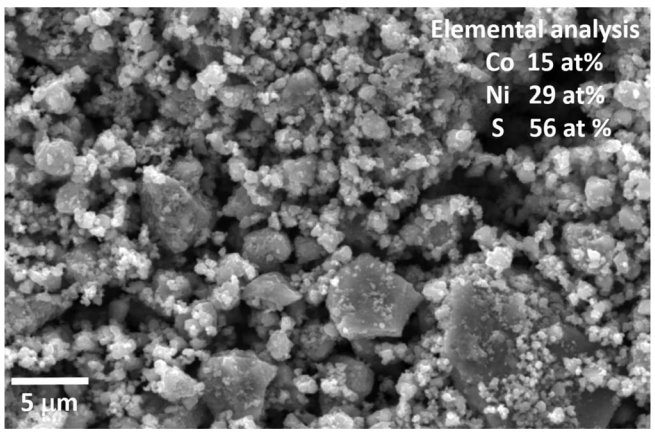

Figure 3. SEM image of $CoNi_2S_4$.

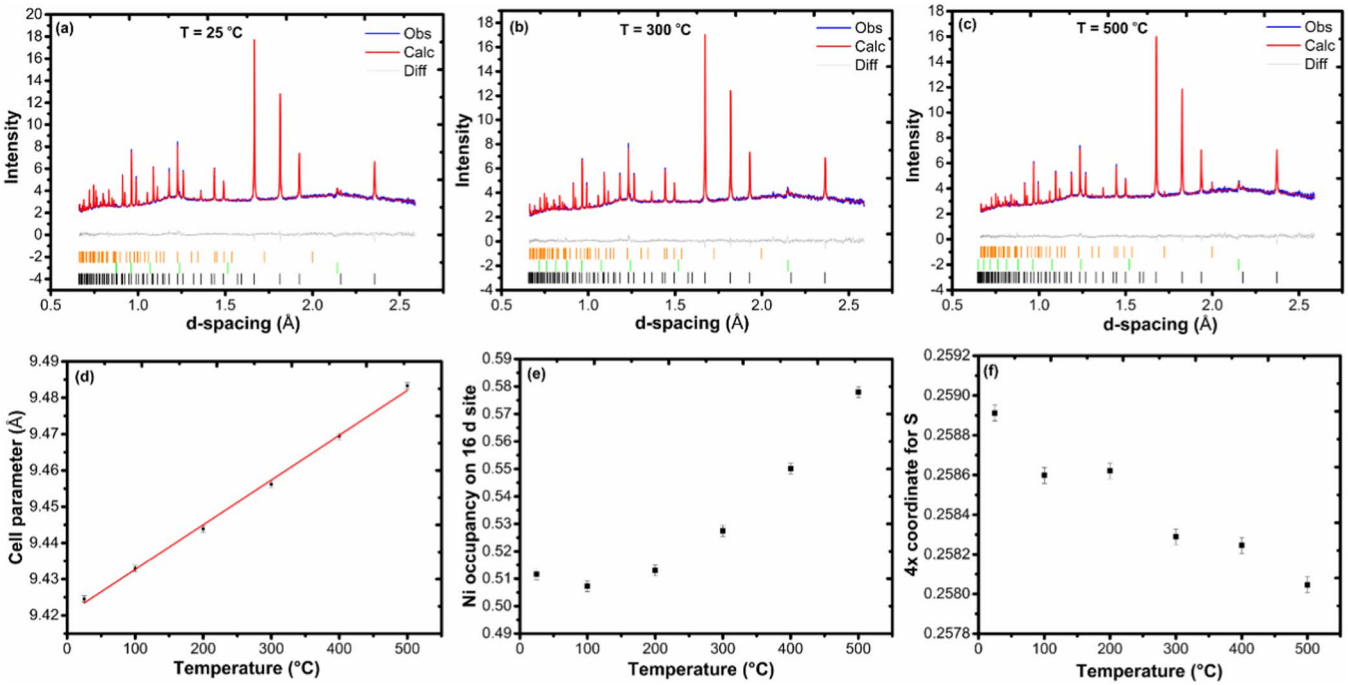

Figure 4. Rietveld fit of inverse spinel model of $CoNi_2S_4$ to powder neutron diffraction data at room temperature (a), at 300°C (b) and at 500°C (c). (Black marks are $CoNi_2S_4$, green marks are vanadium and orange marks are $Ni_{1-x}Co_xS$). Cell parameter of $CoNi_2S_4$ vs temperature from 25°C up to 500°C (d), Ni occupancy vs temperature (e) and '4x' coordinate (for sulfur) vs temperature (f).

shorter duration of our optimized synthesis compared to the existing literature could result in the presence of cation disorder. Neutron diffraction is the ideal tool to study such a material given the difference in neutron scattering lengths of Co and Ni (2.49 and 10.30 fm, respectively).[17] In order to investigate the stability of $CoNi_2S_4$ at elevated temperature and to probe cation (dis)ordering, variable temperature powder neutron diffraction data were collected at temperatures in the range from 25°C–500°C, under vacuum. Sequential refinement of the $CoNi_2S_4$ structural model was carried out in the 25°C to 500°C. Cell parameters, atomic coordinates for sulfur, cation occupancies, an overall isotropic temperature parameter for the cation sites, an isotropic temperature parameter for the sulfur site, 18 background parameters and a scale factor were refined. In initial refinements, cation ordering on the both the 8a and 16d sites was tested across the full temperature range. Refinements of the occupancy of the 8a site found that this site was site fully occupied by nickel and in subsequent refinements the occupancy of the 8a site was fixed to 100% nickel. At room temperature, Rietveld refinement confirms that $CoNi_2S_4$ adopts an inverse spinel structure. Refinement of cation occupancies retains an essentially ordered distribution of cobalt and nickel with no evidence of cation anti-site disorder or non-stoichiometry on the 16d site. This ordering pattern is retained up to 200°C, but above this temperature, there is a gradual increase of nickel on the 16d site with increasing temperature, as shown in Figure 4. This was accompanied by a small decrease in the atomic coordinates of sulfur as these moved closer to ideal 0.25 value. At 500°C, a small amount of secondary phase can be observed in the diffraction pattern and this can be attributed to a "$Ni_{1-x}Co_xS$" $P6_3/mmc$ phase (a = 3.4468(2) Å, c = 5.3787(6) Å). This suggests some sulfur loss under the vacuum conditions of this experiment. The cell parameter of the unit cell increases as the temperature increases as shown in Figure 4. The refined structural parameters of $CoNi_2S_4$ are presented in Table II.

Table II. Selected structural parameters of $CoNi_2S_4$.

Temperature	25°C	300°C	500°C
R_{wp} %	2.25	2.15	2.01
Unit cell a / Å	9.42448(3)	9.45626(4)	9.48343(4)
Ni 16d site occupancy	0.511(5)	0.527(6)	0.578(6)
x 32 e site	0.2589(13)	0.2582(15)	0.2580(17)
Ni (8a)-S (Å)	2.186(2)	2.183(2)	2.185(3)
Ni/Co (16d) -S (Å)	2.2752(11)	2.2884(13)	2.2971(16)

Electrochemical investigation of $CoNi_2S_4$ at 500°C.—$CoNi_2S_4$ was characterized electrochemically by galvanostatic discharge. Discharging was performed at current densities from 15 to 60 mA/cm^2 at 500°C and the results are presented in Figure 5. The cut-off voltage was 1.0 V. At current densities of 15 and 19 mA/cm^2 there is a flat voltage plateau at 1.75 V for x = 1.33 Li, and then a second plateau at 1.50 V for x = 2.66 Li, with a total capacity of 350 mA h g^{-1}. The

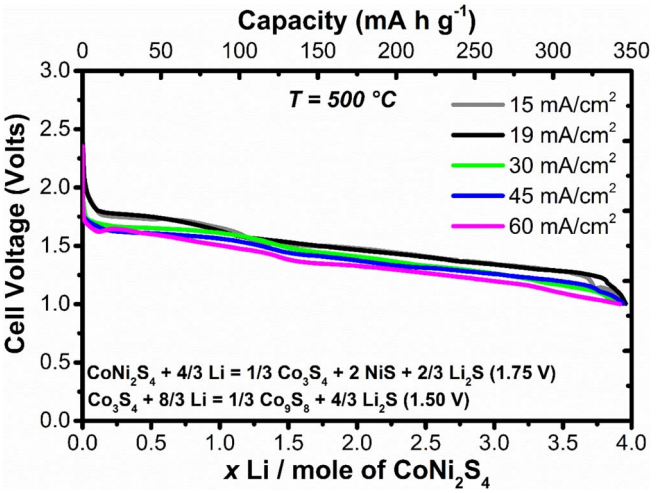

Figure 5. Galvanostatic discharge of $CoNi_2S_4$ at current densities from 15 to 60 mA/cm^2 at 500°C.

Table III. Electrochemical reactions, Voltages, Capacity and Thermal Stability of $CoNi_2S_4$ compared to FeS_2, CoS_2 and NiS_2.

	FeS_2	CoS_2	NiS_2	$CoNi_2S_4$
1st Electrochemical reaction	$FeS_2+3/2Li \rightarrow \frac{1}{2}Li_3Fe_2S_4$	$CoS_2+4/3Li \rightarrow 1/3Co_3S_4+2/3Li_2S$	$NiS_2+2Li \rightarrow NiS+Li_2S$	$CoNi_2S_4+4/3Li \rightarrow 1/3Co_3S_4+2NiS+2/3Li_2S$
Voltage (V) vs Li-Al at 400°C	1.75[6]	1.70[6]	1.74[6]	-
Voltage (V) vs $Li_{13}Si_4$ at 500°C	1.77[19]	1.75[19]	1.76[19]	1.75
2nd Electrochemical reaction	$Li_3Fe_2S_4+Li \rightarrow Li_2FeS_2+FeS+Li_2S$	$Co_3S_4+8/3Li \rightarrow 1/3Co_9S_8+4/3Li_2S$	$7NiS+2Li \rightarrow Ni_7S_6+Li_2S$	$Co_3S_4+8/3Li \rightarrow 1/3Co_9S_8+4/3Li_2S$
Voltage (V) vs Li-Al at 400°C	1.64[6]	1.64[6]	1.58[6]	-
Voltage (V) vs $Li_{13}Si_4$ at 500°C	1.64[19]	1.40[19]	1.60[19]	1.50
3rd Electrochemical reaction	$Li_2FeS_2 \rightarrow Fe+Li_2S+S$	$Co_9S_8+16Li \rightarrow 9Co+8Li_2S$	$3Ni_7S_6+8Li \rightarrow 7Ni_3S_2+4Li_2S$	-
Voltage (V) vs Li-Al at 400°C	1.26[6]	1.37[6]	1.55[6]	-
Voltage (V) vs $Li_{13}Si_4$ at 500°C	1.13[19]	1.25[19]	1.40[19]	-
4th Electrochemical reaction	-	-	$Ni_3S_2+4Li \rightarrow 3Ni+2Li_2S$	-
Voltage (V) vs Li-Al at 400°C	-	-	1.36[6]	-
Voltage (V) vs $Li_{13}Si_4$ at 500°C	-	-	1.25[19]	-
Overall capacity (mA h g^{-1}) (OCV – 1.0 V)	558[6]	598[6]	545[6]	350
Overall capacity (mA h g^{-1}) (OCV – 1.25 V)	390	414	413	318
Thermal stability (°C)	580[22,23]	650[20]	600[21]	550

first plateau corresponds to the electrochemical reaction

$$CoNi_2S_4 + 4/3Li \rightarrow 1/3Co_3S_4 + 2NiS + 2/3Li_2S.$$

The second plateau corresponds to the electrochemical reaction

$$Co_3S_4 + 8/3Li \rightarrow 1/3Co_9S_8 + 4/3Li_2S.$$

At higher current densities of 30, 45, and 60 mA/cm^2 the voltages of these plateau are lower and this is probably due to a higher cell resistance.

The amount of active anode (0.15 g) corresponds to 73 mA h for the discharge plateau from $Li_{13}Si_4$ to Li_7Si_3 which is 0.157 V vs Li metal. The measured capacity of $CoNi_2S_4$ of the first discharge plateau is 17.50 mA h and of the second discharge plateau is 35 mA h. Total of 52.5 mA h, which keeps the discharge as being performed against the 0.157 V Li metal plateau.

$CoNi_2S_4$ exhibits only two electrochemical steps compared to the most commonly used sulfides such as FeS_2, CoS_2 and NiS_2 which are against Li-Al at 400°C[6,18,19] and against $Li_{13}Si_4$ at 500°C as shown in Table III.

$CoNi_2S_4$ has a good thermal stability up to 550°C and this is comparable to that of the well-known materials FeS_2, CoS_2 and NiS_2 as shown in Table III. In the voltage range from OCV 2.58 V to 1.25 V, the $CoNi_2S_4$ has an overall capacity of 318 mA h g^{-1} which is comparable to that of the well-known metal disulfides FeS_2, CoS_2 and NiS_2 (390, 414 and 413 mA h g^{-1}, respectively) as shown in Table III.[6,19,20–23] The advantage of $CoNi_2S_4$ is that this capacity comes from one 'single' discharge process compared to that of MS_2 (M = Fe, Co, Ni) which exhibit 'two' discharge processes. The discharge voltage of $CoNi_2S_4$ decreases gradually from 1.60 V to 1.25 V, unlike in the case of the FeS_2, CoS_2 and NiS_2 which exhibit sharper fall-off in voltage in this region.

$CoNi_2S_4$ has less overall capacity and this is because the $CoNi_2S_4$ does not reduce to the metals Co and Ni at the end of discharge mechanism. The extra capacity obtained in MS_2 comes from voltages below 1.25 V, however, the extra capacity at such low voltage is not useful for practical applications, which means that our $CoNi_2S_4$ exhibits a comparable 'useful' capacity and voltage to the MS_2 cathodes.

Figure 6a shows the PXRD data collected between the first and the second plateaus. PXRD data show that there are peaks from different phases which could be assigned to known crystalline phases in the PDF database. Some peaks could be indexed to a hexagonal unit

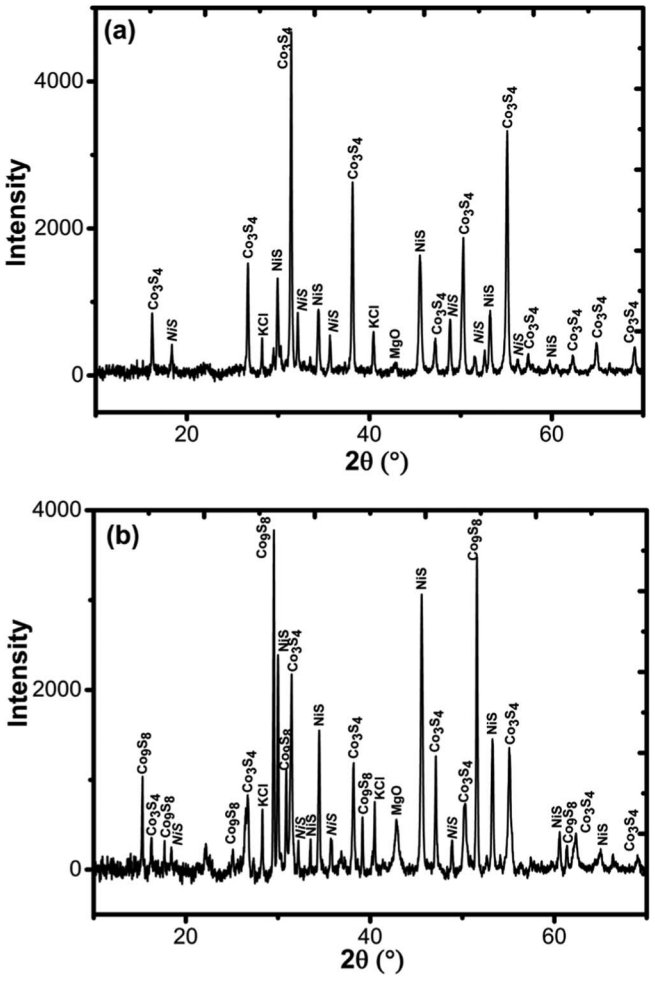

Figure 6. PXRD data collected at room temperature of the cathode following galvanostatic discharge (a) after stopping the discharge between the first and second plateaus and (b) at the end of the galvanostatic discharge at 500°C.

cell, with cell parameters ($a = 3.47(4)$ Å, $c = 5.35(4)$ Å), and space group $P6_3/mmc$ and suggests a NiS phase and not a CoS phase or other phases, as the values are closer to the literature. Also some other peaks could be indexed to a rhombohedral unit cell, with cell parameters ($a = 9.607(3)$ Å, $c = 3.142(10)$ Å) and space group $R3m$ and suggests a *NiS* phase as well. Moreover a cubic phase with space group $Fd\bar{3}m$ and unit cell ($a = 9.402(20)$ Å) suggests a Co_3S_4 phase. Therefore we suggest the formation of NiS and Co_3S_4 as the product of the electrochemical process after the first plateau in the discharge curve. PXRD data was also collected at the end of discharge and are shown in Figure 6b. Data show a hexagonal NiS phase ($a = 3.43(7)$ Å, $c = 5.34(11)$ Å), a rhombohedral *NiS* phase ($a = 9.615(8)$ Å, $c = 3.147(4)$ Å) and also a cubic Co_9S_8 phase ($a = 10.01(9)$ Å). However there are also peaks of Co_3S_4 and peaks of the KCl from the electrolyte and MgO from the separator. Therefore the formation of Li_2S and Co_9S_8 occurs during the electrochemical process at the end of the second plateau. PXRD data is in agreement with the initially suggested equations of the electrochemical reactions, as indicated amount of charge passed on these plateaus.

Conclusions

An improved, shorter synthesis of $CoNi_2S_4$ using a solid state reaction has been reported, with a phase pure material being synthesized at 550°C in just two firing steps. The structure cation order, and thermal stability of $CoNi_2S_4$ has been studied using powder neutron diffraction. The high temperature discharge behavior of $CoNi_2S_4$ is presented in this work. At a temperature of 500°C the value of the working voltage plateau was recorded at different current densities from 15 to 60 mA/cm^2 and a capacity of 350 mA h g^{-1} was achieved. A potential value of 1.75 V [$x = 4/3$ Li] and of 1.50 V [$x = 8/3$ Li] vs $Li_{13}Si_4$ for $CoNi_2S_4$ was found at 500°C. This material could be a promising candidate for Li thermal battery applications as it exhibits a similar behavior to the most commonly used sulfides FeS_2, CoS_2 and NiS_2 and all its properties are comparable to that of the well-known metal disulfides.

Acknowledgments

We acknowledge support and contribution from AWE Plc for this work. We thank the STFC for neutron diffraction beam-time and Dr. D. Fortes for assistance on HRPD. We also thank Stewart Dickson for his help.

References

1. R. A. Guidotti and P. Masset, *J. Power Sources*, **161**, 1443 (2006).
2. P. Masset and R. A. Guidotti, *J. Power Sources*, **164**, 397 (2007).
3. R. A. Sharma and F. N. Seefurth, *J. Electrochem. Soc.*, **124**(8), 1207 (1977).
4. C. J. Wen and R. A. Huggins, *J. Solid State Chem.*, **37**, 271 (1981).
5. J. Sangster and A. D. Pelton, *J. Phys. Chem. Ref. Data*, **16**(3), 509 (1987).
6. S. K. Preto, Z. Tomczuk, S. von Winbush, and M. F. Roche, *J. Electrochem. Soc.*, **130**, 264 (1983).
7. R. A. Guidotti, 27 International SAMPE Technical Conference, Abuquerque, NM October 9–12, (1995).
8. R. A. Guidotti and F. W. Reinhardt, Sandia National Laboratory, NM 87185-0614 (1996).
9. Lin Mei, Ting Yang, Cheng Xu, Ming Zhang, Libao Chen, Qiuhong Li, and Taihong Wang, *Nano Energy*, **3**, 36 (2014).
10. Shaolan Wang, Wei Li, Lipeng Xin, Ming Wu, and Xiaojie Lou, *RSC Adv*, **6**, 42633 (2016).
11. Weimin Du, Zhaoqiang Zhu, Yanbin Wang, Junning Liu, Wenjie Yang, Xuefeng Qian, and Huan Pang, *RSC Adv*, **4**, 6998 (2014).
12. Huang Chunghis and O Knop, *Canadian Journal of Chemistry*, **49**, 598 (1971).
13. A. C. Larson and R. B. Von Dreele, "General Structure Analysis System (GSAS)", Los Alamos National Laboratory Report LAUR 86 - 748 (1994).
14. B. H. Toby, EXPGUI, a graphical user interface for GSAS, *J. Appl. Cryst.*, **34**, 210 (2001).
15. L. Mancic, Z. Marinkovic, P. Vulic, C. Moral, and O. Milosevic, *Nanophased Powder, Sensors*, **3**, 415 (2003).
16. K. Matsuda, T. Matsuki, I. Mullerova, L. Frank, and S. Ikeno, *Materials Transactions*, **47**(7), 1815, (2006).
17. V. F. Sears, *Neutron News*, **3**(3), 29 (1992).
18. P. J. Masset and R. A. Guidotti, *Journal of Power Sources*, **177**, 595 (2008).
19. P. J. Masset and R. A. Guidotti, *Journal of Power Sources*, **178**, 456 (2008).
20. H. Rau, *J. Phys. Chem. Solids*, **37**, 931 (1976).
21. R. A. Guidotti, P. J. Nigrey, F. W. Reinhardt, and J. G. Odinek, *Proceedings of the 40th Power Sources Conference*, 250 (2002).
22. M. C. Hash, J. A. Smaga, R. A. Guidotti, and F. W. Reinhardt, *Proceedings of the 8th International Symposium on Molten Salts*, 228 (1992).
23. I. C. Hoare, H. J. Hurst, W. I. Stuart, and T. J. White, *J. Chem. Soc. Faraday Trans.*, **184**(9), 3071 (1988).